

RESEARCH ARTICLE

Synthesis and bioevaluation of *N*,4-diaryl-1,3-thiazole-2-amines as tubulin inhibitors with potent antiproliferative activity

Maolin Sun¹✉, Qile Xu¹✉, Jingwen Xu², Yue Wu¹, Yueting Wang¹, Daiying Zuo², Qi Guan¹, Kai Bao^{1,3}, Jian Wang^{1*}, Yingliang Wu², Weige Zhang^{1*}

1 Key Laboratory of Structure-Based Drug Design and Discovery, Ministry of Education, Shenyang Pharmaceutical University, Shenyang, China, **2** Department of Pharmacology, Shenyang Pharmaceutical University, Shenyang, China, **3** Gordon Center for Medical Imaging, Division of Nuclear Medicine and Molecular Imaging, Department of Radiology, Massachusetts General Hospital and Harvard Medical School, Boston, Massachusetts, United States of America

✉ These authors contributed equally to this work.
* zhangweige2000@sina.com (WZ); jianwang@syphu.edu.cn (JW)



OPEN ACCESS

Citation: Sun M, Xu Q, Xu J, Wu Y, Wang Y, Zuo D, et al. (2017) Synthesis and bioevaluation of *N*,4-diaryl-1,3-thiazole-2-amines as tubulin inhibitors with potent antiproliferative activity. PLoS ONE 12 (3): e0174006. <https://doi.org/10.1371/journal.pone.0174006>

Editor: Sandra B. Gabelli, Johns Hopkins University School of Medicine, UNITED STATES

Received: July 23, 2016

Accepted: March 1, 2017

Published: March 23, 2017

Copyright: © 2017 Sun et al. This is an open access article distributed under the terms of the [Creative Commons Attribution License](https://creativecommons.org/licenses/by/4.0/), which permits unrestricted use, distribution, and reproduction in any medium, provided the original author and source are credited.

Data Availability Statement: All relevant data are within the paper and its Supporting Information file.

Funding: This work was supported by the the National Natural Science Foundation of China (81502932), State Key Laboratory of Natural Medicines and Active Substance (No. GTZK201603), the Programme for Innovative Research Team of the Ministry of Education and the Programme for Liaoning Innovative Research Team in University. The funders had no role in

Abstract

A series of *N*,4-diaryl-1,3-thiazole-2-amines containing three aromatic rings with an amino linker were designed and synthesized as tubulin inhibitors and evaluated for their antiproliferative activity in three human cancer cell lines. Most of the target compounds displayed moderate antiproliferative activity, and *N*-(2,4-dimethoxyphenyl)-4-(4-methoxyphenyl)-1,3-thiazol-2-amine (**10s**) was determined to be the most potent compound. Tubulin polymerization and immunostaining experiments revealed that **10s** potently inhibited tubulin polymerization and disrupted tubulin microtubule dynamics in a manner similar to CA-4. Moreover, **10s** effectively induced SGC-7901 cell cycle arrest at the G₂/M phase in both concentration- and time-dependent manners. The molecular docking results revealed that **10s** could bind to the colchicine binding site of tubulin.

Introduction

Microtubules are key structural components in eukaryotic cells and play a crucial role in a number of cellular functions, including regulation of motility, cell division, organelle transport, maintenance of cell morphology and signal transduction [1,2]. Tubulin-binding drugs disrupt microtubule/tubulin dynamics by binding to distinct sites such as taxol, vinca alkaloid and colchicine binding sites and arrest cells during mitosis, leading to cell death [3–5]. In contrast to macromolecular paclitaxel and vinblastine, most novel colchicine binding site inhibitors (CBSIs) have high potency, relatively simple and diverse chemical structures for optimization, and selective toxicity toward tumor vasculature [6]. Given the success of paclitaxel and vinblastine, research efforts have been focused on developing CBSIs for cancer treatment, and a number of effective CBSIs are currently being investigated in clinical studies [7]. Some representative CBSIs include the natural products colchicine (**1**), combretastatin A-4 (CA-4, **2**) and nocodazole (**3**), shown in Fig 1A [8–12]. Phenstatin (**4**) is a CA-4 analog in which the double bond of CA-4 is replaced with a carbonyl linker [13]. The common structural

study design, data collection and analysis, decision to publish, or preparation of the manuscript.

Competing interests: The authors have declared that no competing interests exist.

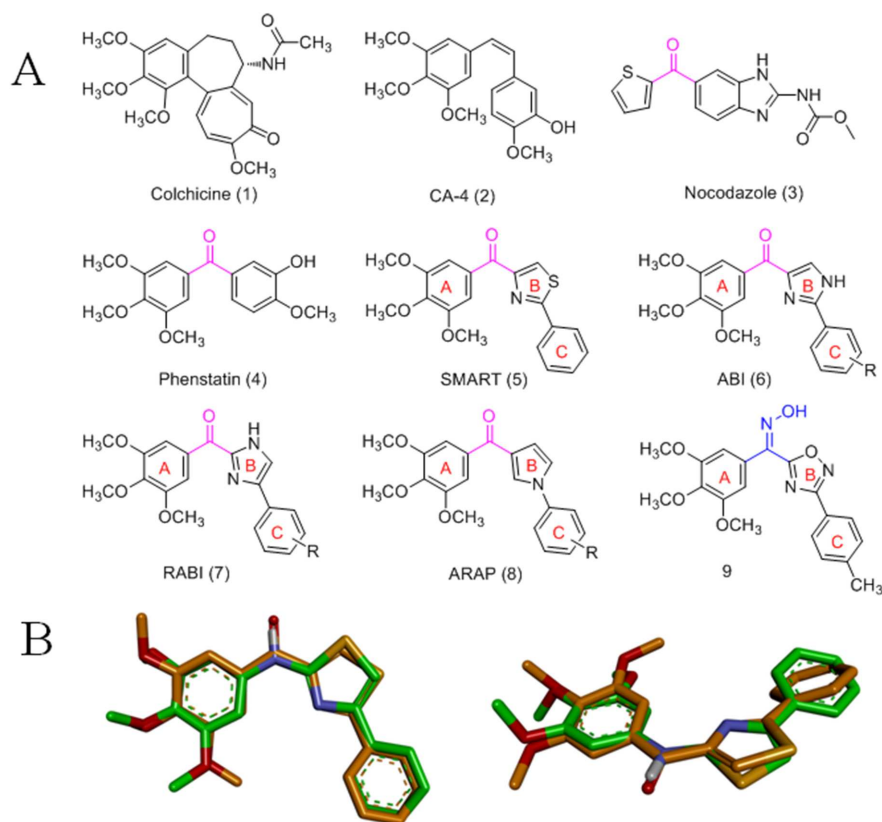


Fig 1. (A) Structures of known tubulin inhibitors. (B) Superposition of the skeletal structure of target compounds 10a-m and SMART. All density functional theory calculations and geometry optimizations were performed using the Gaussian 09 software.

<https://doi.org/10.1371/journal.pone.0174006.g001>

features of CBSIs include the 3,4,5-Trimethoxyphenyl unit and the appropriate distance and certain dihedral angle between the aromatic rings. These were proposed as important structural features that are responsible for their antiproliferative and antitubulin activities [6].

The CBSIs 4-substituted methoxybenzoyl-aryl-thiazole (SMART, 5), 2-aryl-4-benzoyl-imidazole (ABI, 6), 4-aryl-2-benzoyl-imidazoles (RABI, 7) and 3-aryl-1-arylpyrrole (ARAP, 8) are the representative synthetic CBSIs that exhibit potent antiproliferative activity (Fig 1A) [14–17]. Furthermore, a set of oxadiazole CBSIs with an oxime linker between the A-ring and the B-ring was previously reported by our group (9, Fig 1A) [18]. The structures of these CBSIs feature three aromatic rings (A-, B- and C- rings) and an sp^2 hybridized linker between the A-ring and B-ring (Fig 1A).

2-Aminothiazoles and derivatives are seen in many bioactive scaffolds and exhibit a variety of biological properties, including anticancer activity [19]. Furthermore, CBSIs containing an sp^3 amino linker have also been reported [20]. In our continued research into novel CBSIs [18, 21, 22], we hypothesized that the sp^2 linker between the A- and B-rings could be replaced by a sp^3 amino linker and that the substitutions on the A- and C-rings could be different groups. As expected from calculations using the Gaussian 09 software, the skeletal structure of target compounds superimposed well with that of SMART (Fig 1B). In this study, we report the verification of our hypothesis through the synthesis and biological evaluation of the designed target CBSIs (Table 1). In addition, the preliminary structure-activity relationships and the mechanism of the representative compound 10s are investigated and determined.

Table 1. Molecular structures of compounds 10a-v.

Structures	R ₁	R ₂	R ₃	R ₄	R ₅	R ₆	R ₇	R ₈	R ₉
10a	H	OCH ₃	OCH ₃	OCH ₃	H	H	CH ₃	H	H
10b	H	OCH ₃	OCH ₃	OCH ₃	H	H	OCH ₃	H	H
10c	H	OCH ₃	OCH ₃	OCH ₃	H	H	F	H	H
10d	H	OCH ₃	OCH ₃	OCH ₃	H	H	Cl	H	H
10e	H	OCH ₃	OCH ₃	OCH ₃	H	H	Br	H	H
10f	H	OCH ₃	OCH ₃	OCH ₃	H	H	NO ₂	H	H
10g	H	OCH ₃	OCH ₃	OCH ₃	H	H	OCH ₃	OCH ₃	H
10h	H	OCH ₃	OCH ₃	OCH ₃	H	H	OCH ₃	F	H
10i	H	OCH ₃	OCH ₃	OCH ₃	H	H	OCH ₃	NO ₂	H
10j	H	OCH ₃	OCH ₃	OCH ₃	H	H	OCH ₃	NH ₂	H
10k	H	OCH ₃	OCH ₃	OCH ₃	H	H	OCH ₃	OBn	H
10l	H	OCH ₃	OCH ₃	OCH ₃	H	H	OCH ₃	OH	H
10m	H	OCH ₃	OCH ₃	OCH ₃	H	H	F	F	H
10n	H	OCH ₃	H	OCH ₃	H	H	OCH ₃	H	H
10o	H	H	OCH ₃	H	H	OCH ₃	OCH ₃	OCH ₃	H
10p	H	CH ₃	CH ₃	H	H	H	OCH ₃	NO ₂	H
10q	H	CH ₃	CH ₃	H	H	H	OCH ₃	NH ₂	H
10r	OCH ₃	H	OCH ₃	H	H	H	CH ₃	H	H
10s	OCH ₃	H	OCH ₃	H	H	H	OCH ₃	H	H
10t	OCH ₃	H	OCH ₃	H	H	H	OCH ₃	H	OCH ₃
10u	OCH ₃	H	OCH ₃	H	CH ₃	H	OCH ₃	H	H
10v	OCH ₃	H	OCH ₃	H	Ac	H	OCH ₃	H	H

<https://doi.org/10.1371/journal.pone.0174006.t001>

Results and discussion

Chemistry

The target compounds contained a 2-aminothiazole (2-AT) scaffold that has been widely used by medicinal chemists in drug discovery research. Few drugs containing a 2-AT core (e.g., mirabegron, riluzole, cefotaxime and meloxicam) have been launched in the market [23]. In our designed compounds, the amino group played a vital role in maintaining the spatial configuration and biological activity of target compounds. Target compounds were prepared as outlined in Fig 2. In brief, the condensation of commercially aniline derivatives **11** with carbon disulfide in the presence of triethylamine gave the corresponding dithiocarbamates **12** at room temperature at an 80–96% yield [24]. Subsequently, dithiocarbamates **12** were used for the synthesis of aryl thioamides **14** using an efficient one-pot method [25]. More speculatively, dithiocarbamates **12** in ethyl acetate were incubated with triethylamine at 0°C. Iodine was then added pinch-wise over a period of 15 minutes to yield phenylisothiocyanates **13**, which were then reacted with ammonium hydroxide to obtain the key intermediates aryl thioureas **14** at room temperature. Alternatively, the commercially available starting acetophenones **15** were subjected to α -bromination with copper dibromide in refluxing chloroform-ethyl acetate to produce α -bromoacetophenones **16** at 75–95% yield. Finally, α -bromoacetophenones **16** were reacted with aryl thioureas **14** to generate the desired compounds **10a-t** in ethanol within 5 min under microwave irradiation (150 W, 80°C) in the absence of catalysts [26]. The compound **10u** was obtained by a simple reaction of the compound **10s** with methyl iodide in anhydrous DMF, and the compound **10v** was obtained by an acetylation reaction of compound **10s** with acetic anhydride.

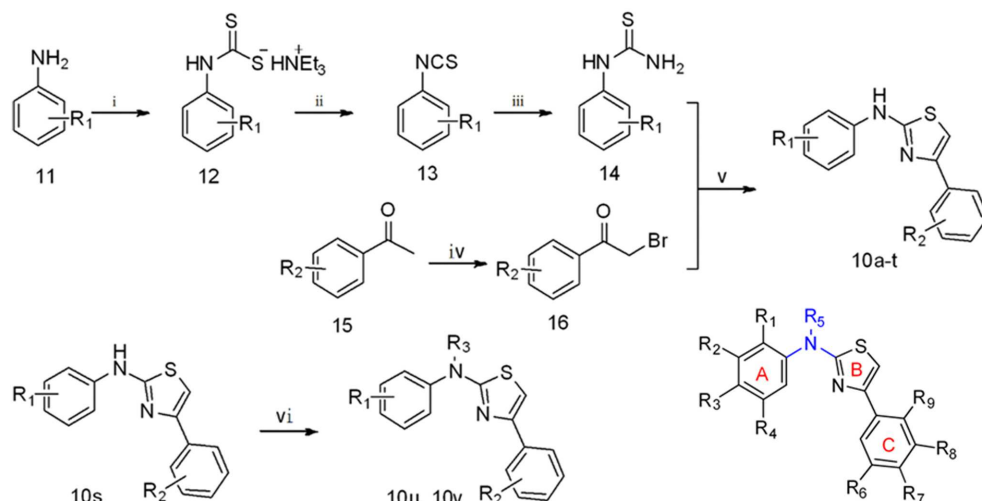


Fig 2. Reagents and conditions. (i) CS_2 , Et_3N , Et_2O , 25°C ; (ii) I_2 , Et_3N , EtOAc , 0°C ; (iii) $\text{NH}_3\cdot\text{H}_2\text{O}$; (iv) CuBr_2 , CHCl_3 , EtOAc ; (v) EtOH , MW 80°C ; (vi) 1) CH_3I , DMF , 25°C or 2) Ac_2O , 50°C .

<https://doi.org/10.1371/journal.pone.0174006.g002>

Biological studies

In vitro antiproliferative activity. Gastric cancer and lung cancers are the two most common cancers and the two most frequent causes of cancer-related deaths [27]. HT-1080 is a fibrosarcoma cell line which has been used extensively in biomedical research [28]. So we chose these three human cancer cell lines (gastric adenocarcinoma SGC-7901 cells, lung adenocarcinoma A549 cells and fibrosarcoma HT-1080 cells) for antiproliferative activity. To evaluate the ability of various 2-aminothiazole derivatives to inhibit cancer cell growth, the target compounds **10a-v**, reference compounds CA-4 (**2**), nocodazole (**3**) and SMART (**5**) were screened for antiproliferative activity in three human cancer cell lines using a standard MTT assay (Table 2). The reported IC_{50} values are the average of at least three independent experiments. As illustrated in Table 2, most of the target compounds showed moderate antiproliferative activities with potencies in the μM range. Comparison of the IC_{50} values of the corresponding compounds **10a-m** with 3,4,5-trimethoxy (R_2 , R_3 , $\text{R}_4 = \text{OMe}$) substitution revealed that only the 3-hydroxy-4-methoxy-substituted compound **10l** significantly inhibited growth of the HT-1080 cell line at sub-micromolar concentrations. The target compounds contain halide substituents that has been widely used by medicinal chemists in CBSI research, so we synthesis these compounds to evaluate the potential antiproliferative activities. Unexpectedly, we found that these compounds (**10c**, **10d**, **10e**, **10h**, **10m**) showed only moderate antiproliferative activities. Interestingly, the most significant enhancement of antiproliferative activity was observed in the amino-linked compounds where the A ring accommodates the 2,4-dimethoxy substitutions. *N*-(2,4-dimethoxyphenyl)-4-(4-methoxyphenyl)-1,3-thiazol-2-amine **10s** exhibited the most potent antiproliferative activity, with IC_{50} values between 0.36 and 0.86 μM in the three cancer cell lines. However, the introduction of a methyl (**10u**) or acetyl (**10v**) group at the N position of the 2-aminothiazole skeleton resulted in reduced activity compared to the corresponding compound (**10s**).

Tubulin polymerization. CBSIs exert their biological activity by inhibiting tubulin assembly. To confirm that the antiproliferative activities of these compounds were related to the microtubule system, the most active compound **10s** was evaluated for tubulin polymerization inhibition compared to the positive control CA-4 and the negative control paclitaxel. As

Table 2. Antiproliferative activity of compounds 10a-v, CA-4 (2), Nocodazole (3) and SMART (5).

Compounds	Antiproliferative activity (IC ₅₀ ± SD, μM) ^a		
	SGC-7901	A549	HT-1080
10a	1.12 ± 0.13	1.32 ± 0.12	1.17 ± 0.19
10b	7.72 ± 0.26	26.8 ± 2.2	26.8 ± 1.2
10c	27.7 ± 4.9	16.1 ± 1.1	7.40 ± 0.42
10d	8.22 ± 0.17	1.80 ± 0.19	1.26 ± 0.25
10e	2.30 ± 0.32	3.18 ± 0.16	6.61 ± 0.18
10f	>100	23.6 ± 2.3	>100
10g	4.89 ± 0.15	5.36 ± 0.16	6.94 ± 0.14
10h	4.92 ± 0.12	6.17 ± 0.32	5.48 ± 0.21
10i	9.11 ± 0.62	9.25 ± 0.33	6.24 ± 0.24
10j	1.17 ± 0.17	6.54 ± 0.16	4.69 ± 0.62
10k	13.0 ± 2.1	13.1 ± 1.1	5.01 ± 0.18
10l	1.36 ± 0.09	3.21 ± 0.17	0.77 ± 0.11
10m	10.1 ± 1.1	26.4 ± 1.3	8.46 ± 0.17
10n	0.82 ± 0.06	9.62 ± 0.17	3.36 ± 0.11
10o	19.5 ± 2.4	17.7 ± 1.6	12.7 ± 1.9
10p	9.89 ± 0.18	12.8 ± 1.3	25.8 ± 3.5
10q	14.8 ± 1.5	10.9 ± 3.2	4.89 ± 0.25
10r	1.6 ± 2.2	1.82 ± 0.12	1.95 ± 0.13
10s	0.36 ± 0.19	0.86 ± 0.07	0.58 ± 0.13
10t	10.1 ± 1.0	11.4 ± 1.3	2.46 ± 0.17
10u	28.2 ± 1.9	19.0 ± 2.0	9.39 ± 0.21
10v	23.2 ± 0.11	35.7 ± 0.08	56.6 ± 1.0
CA-4 (2) ^b	0.025 ± 0.012	0.019 ± 0.011	0.032 ± 0.006
Nocodazole (3) ^b	0.24 ± 0.07	0.15 ± 0.09	0.12 ± 0.08
SMART (5) ^b	0.045 ± 0.013	0.059 ± 0.012	0.032 ± 0.009

^a IC₅₀: Concentration of the compound (μM) that resulted in 50% cell growth inhibition after 72 h of drug exposure, as determined by the MTT assay. Each experiment was carried out in triplicate.

^b Used as a positive control.

<https://doi.org/10.1371/journal.pone.0174006.t002>

shown in Fig 3, both CA-4 and 10s inhibited tubulin assembly, and compound 10s inhibited tubulin polymerization in a dose-dependent manner. However, compound 10s displayed less active antitubulin activity than did CA-4 (IC₅₀ = 26.8 μM and 0.64 μM, respectively). In contrast, paclitaxel enhanced the rate of tubulin polymerization compared with untreated cells. These results suggested that compound 10s interfered with microtubule polymerization.

Analysis of immunofluorescence staining. Colchicine binding site inhibitors could inhibit tubulin assembly and suppress microtubule formation. With the goal of ascertaining the mechanism of action of compound 10s, we decided to use a 0.72 μM drug concentration for the cell microtubule organization studies. As shown in Fig 4, the fibrous microtubules (green) and the cell nucleus (blue) were visualized upon the immunofluorescence staining of SGC-7901 cells. These results implied that 10s and CA-4 induced significant defects in tubulin assembly in the treated cells, leading to the formation of abnormal mitotic spindles in comparison with the control. These results further confirmed that tubulin was the molecular target for compound 10s.

Cell cycle study. Because tubulin inhibitors can arrest dividing cells in the G2/M phase of the cell cycle, the effect of 10s on the cell cycle progression of SGC-7901 cells was investigated

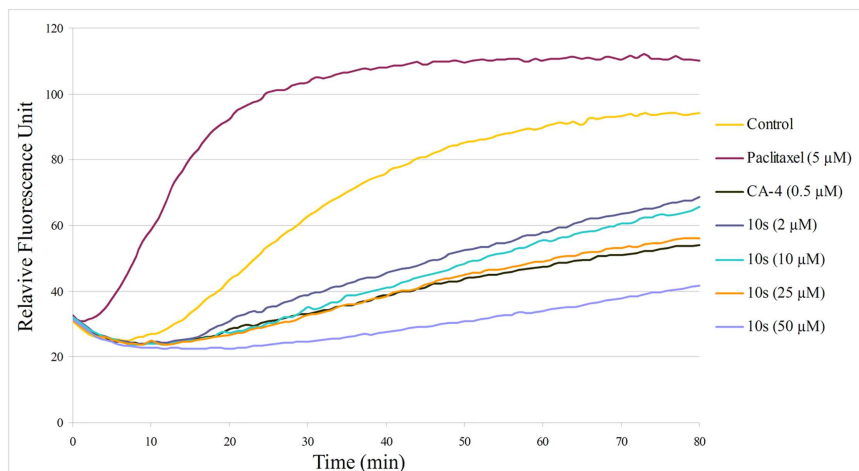


Fig 3. Effects of 10s on tubulin polymerization. Tubulin was pre-incubated for 1 min with 10s at 2 μM, 10 μM, 25 μM and 50 μM, CA-4 at 0.5 μM, paclitaxel at 5 μM or vehicle DMSO (control) at room temperature before GTP was added to start the tubulin polymerization reactions. The reaction was monitored at 37°C.

<https://doi.org/10.1371/journal.pone.0174006.g003>

by flow cytometry analysis. As demonstrated in Fig 5A, 10s caused a dramatic increase in G2/M phase cell counts in a concentration-dependent manner. Furthermore, treatment of SGC-7901 cells with 10s (0.72 μM) or CA-4 (0.05 μM) from 6 to 24 h induced a dramatic increase in

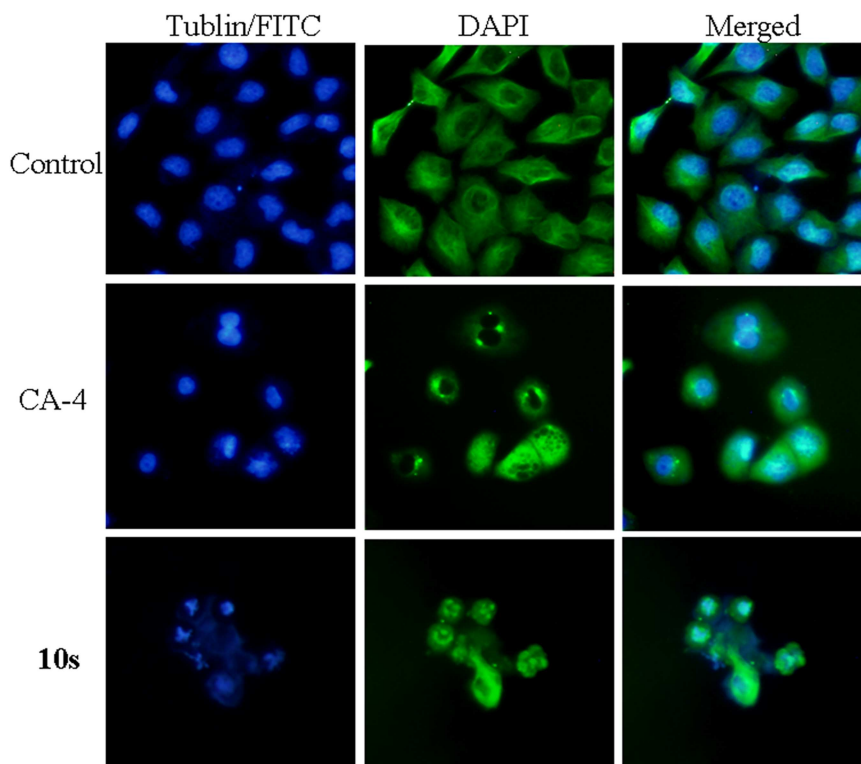


Fig 4. Immunostaining of tubulin assembly in SGC-7901 cells. SGC-7901 cells were treated with 10s (0.72 μM) for 48 h. Tubulin assembly was stained with FITC (left panel) and DAPI (middle panel). A merge of the two panels is shown on the right. Images were taken using a confocal microscope.

<https://doi.org/10.1371/journal.pone.0174006.g004>

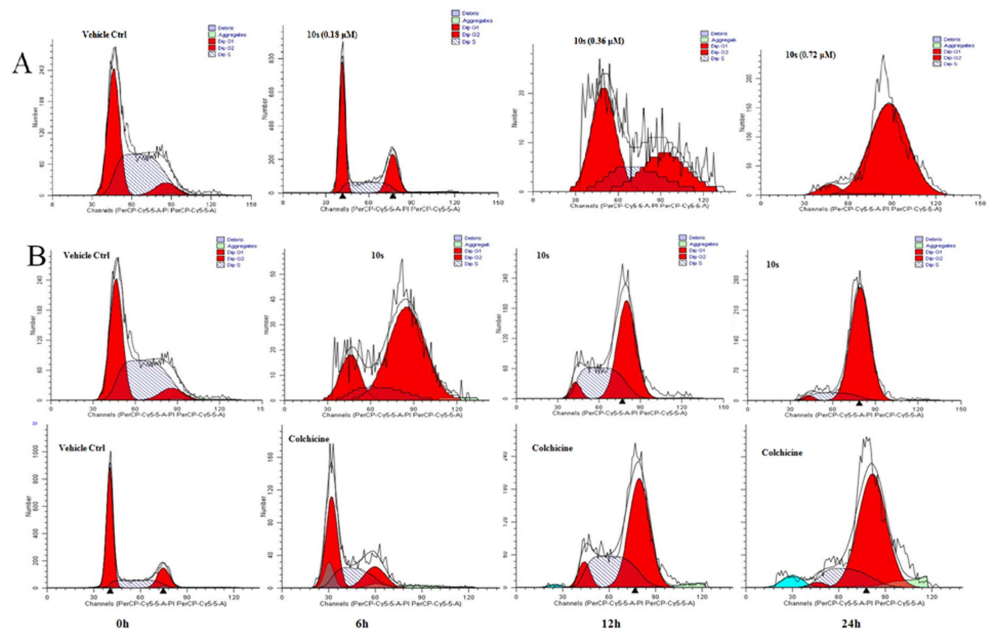


Fig 5. (A) **10s** caused G2/M phase arrest in a concentration-dependent manner in SGC-7901 cells. Cells were treated with **10s** (0.18, 0.36, 0.72 μ M) for 24 h. (B) **10s** and CA-4 induced G2/M phase arrest in a time-dependent manner. SGC-7901 cells were treated with **10s** (0.72 μ M) or CA-4 (0.05 μ M) for 6, 12 and 24 h.

<https://doi.org/10.1371/journal.pone.0174006.g005>

the number of cells in the G2/M phase in a time-dependent manner. These results further demonstrated that **10s** was a tubulin inhibitor.

Molecular modeling. Molecular modeling studies were performed to investigate the potential binding ability of the most active compound **10s** and a moderate compound **10u** to the colchicine binding site of α - and β -tubulin. The molecular modeling study was performed using the CDOCKER protocol in Discovery Studio 3.0 with the default settings to predict the binding mode of our ligand (PDB: 3HKD). These studies showed that **10s**, **10u** and SMART can occupy the colchicine binding site of tubulin (Fig 6). The trimethoxyphenyl moiety of SMART and the dimethoxyphenyl moiety of **10s** and **10u** in the A-rings extended toward the

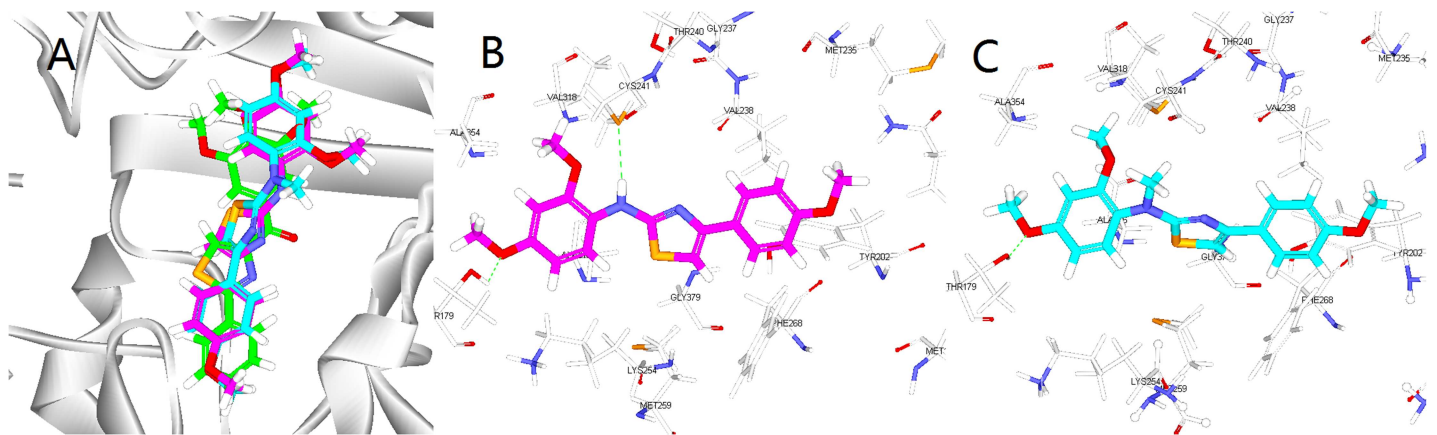


Fig 6. (A). The binding mode of compound **10s** (violet), **10u** (cyan) and SMART (green) in the colchicine binding site of tubulin. (B). Overlay of **10s** in the binding site. Hydrogen bonds are shown using green dashed lines and the distance is less than 3 Å. (C). Overlay of **10u** in the binding site.

<https://doi.org/10.1371/journal.pone.0174006.g006>

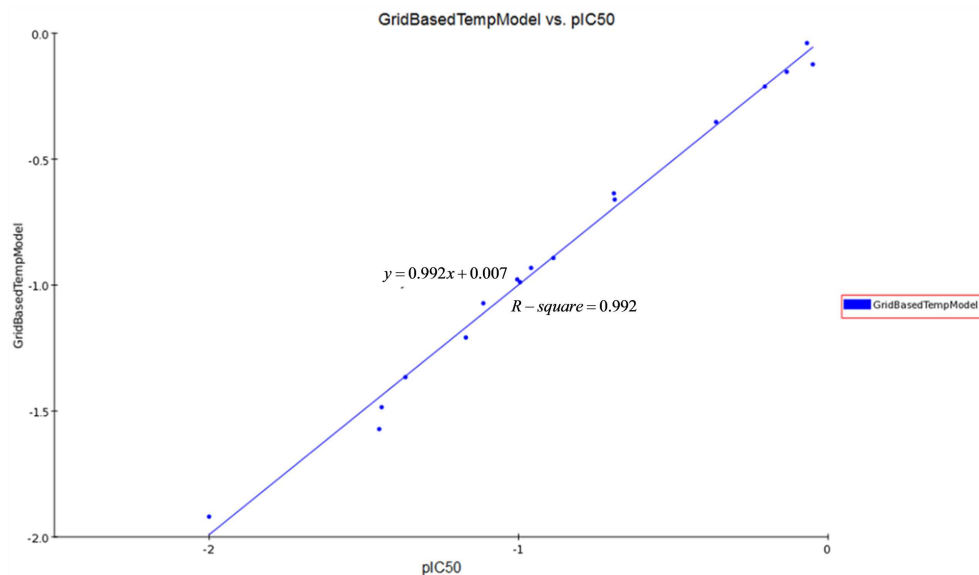


Fig 7. We used a linear fitting curve to compare the predicted pIC₅₀ values (modeled based on a known dataset of 21 defined compounds in SGC-7901 cells) with the experimental pIC₅₀ values. $y = 0.992x + 0.007$, R -square = 0.992.

<https://doi.org/10.1371/journal.pone.0174006.g007>

α - and β -tubulin interfaces. Several amino acids of β -tubulin formed hydrophobic interactions with compounds **10s** and **10u**. The thiol group of Cys β 241 formed a hydrogen bond with the nitrogen atom of the amino linker and the methoxy oxygen atom in ring A of **10s** formed a hydrogen bond with the hydroxyl group of Thr α 179. However, the thiol group of Cys β 241 could not form a hydrogen bond with the nitrogen atom of **10u** due to the methyl group on nitrogen atom. This may be the reason that the activities of **10u** was less active than **10s**. The docking study results revealed that **10s** could bind the colchicine binding site of tubulin.

QSAR model. By using the Create 3D QSAR protocol in Discovery Studio 3.0, twenty-one synthesized compounds with definite IC₅₀ values against SGC-7901 were selected as the model dataset. By convention, we used the pIC₅₀ scale ($-\log$ IC₅₀), in which higher values indicate exponentially greater potency, to measure inhibitory activity. The training set and testing set were chosen by the Diverse Molecules method in Discovery Studio 3.0. To ensure a good alignment, we chose the alignment conformation of each molecule with the lowest energy in the docked results of the CDocker protocol. We applied the alignment of the substructure **10a** before building the QSAR model. The correlation coefficient r^2 between the observed activity of the testing set and the training set was found to be 0.992; therefore, the QSAR model that we built was acceptable (greater than 0.5, Fig 7). Additionally, the molecules that aligned with the iso-surfaces of the 3D-QSAR model (Organic & Biomolecular Chemistry Page 10 of 349 coefficients) on Van der Waals grids (Fig 8A) and electrostatic potential grids (Fig 8B) were listed. Our electrostatic map indicated red contours around regions where high electron density (negative charge) was expected to increase activity, and blue contours represented areas where low electron density (partial positive charge) was expected to increase activity. Similarly, our steric map indicated areas where steric bulk was predicted to increase (green) or decrease (yellow) activity. It was widely acceptable that a better inhibitor based on the 3D QSAR model should have stronger Van der Waals attractions in the green areas and a polar group in the blue electrostatic potential areas (which were dominant close to the skeleton). Thus, this promising model would provide a guideline to design and optimize more

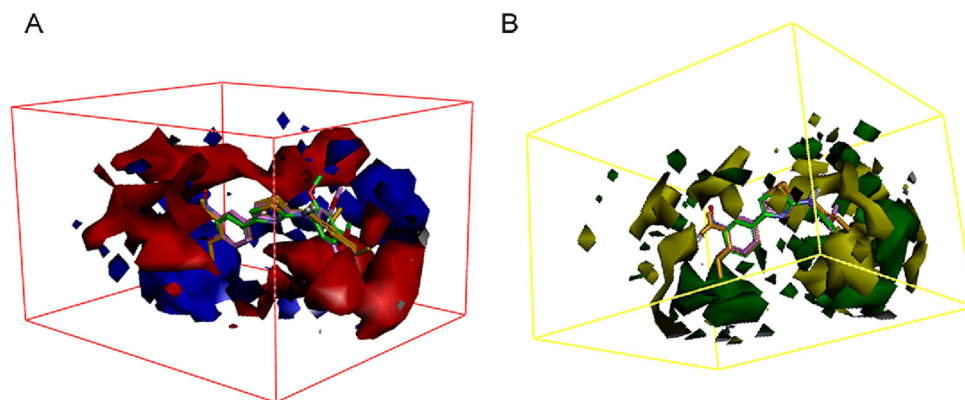


Fig 8. (A). 3D-QSAR model coefficients on electrostatic potential grids. Blue represents positive coefficients; red represents negative coefficients. (B). 3D-QSAR model coefficients on Van der Waals grids. Green represents positive coefficients; yellow represents negative coefficients. (For interpretation of the references to color in this figure legend, the reader is referred to the web version of this article.)

<https://doi.org/10.1371/journal.pone.0174006.g008>

effective tubulin inhibitors based on the *N*,4-diaryl-1,3-thiazole-2-amines skeleton and pave the way for us to further study these compounds in the future.

Conclusions

In summary, we designed and synthesized a series of *N*,4-diaryl-1,3-thiazole-2-amines containing three aromatic rings with an amino linker as novel CBSIs. Most of the target compounds showed moderate anti-proliferative activity in different cancer cells lines with potencies in the μM range. Among them, *N*-(2,4-dimethoxyphenyl)-4-(4-methoxyphenyl)-1,3-thiazol-2-amine, **10s**, was found to be the most potent compound with IC_{50} values at the submicromolar level in three human cancer cell lines. Tubulin polymerization and immunostaining experiments revealed that **10s** potently inhibited tubulin polymerization and disrupted tubulin microtubule dynamics in a manner similar to CA-4. Moreover, **10s** effectively induced SGC-7901 cell cycle arrest at the G_2/M phase in both concentration- and time-dependent manners. Molecular docking results revealed that **10s** could bind the colchicine binding site of tubulin. Taken together, the present study indicates that the utilization of an sp^3 amino linker to replace the sp^2 carbonyl linker can be one of the future directions of novel CBSI synthesis and is deserving of further study. Investigation of the modification of these novel CBSIs and mechanistic studies for anticancer properties are underway in our lab. We will continue to optimize and refine the modification of these compounds and will then select one or two active compounds for in vivo testing.

Experimental section

Chemistry

All solvents and chemical materials were obtained from commercially available sources and were used without purification. The microwave reactions were performed on a discover-sp single mode microwave reactor from CEM Corporation. The progress of reactions was monitored by TLC using silica gel plates under UV light. NMR spectra were recorded on a Bruker AVANCE 400, or 600 spectrometer (^1H , 400 MHz, 600 MHz; ^{13}C , 100 MHz, 150 MHz), in CDCl_3 or DMSO-d_6 (TMS was used as an internal standard). Chemical shifts are expressed as parts per million downfield from tetramethylsilane. Mass spectra (MS) were measured on an Agilent 1100-sl mass spectrometer with an electrospray ionization source. Melting points were measured on a hot stage microscope (X-4, Beijing Taike Ltd.) and are uncorrected.

General synthetic procedures for *N*,4-diaryl-1,3-thiazole-2-amines 10a-v. The α -bromoketones **16** (1.0 mmol) and aryl thioamides **14** (1.0 mmol) were dissolved in ethanol (5 mL). The mixture was heated to 80 °C for 5 min under microwave irradiation (discover-sp, CEM Corporation, 150 W). After the reaction was completed, the mixture was poured into water and extracted with methylene chloride. The organic layer was washed with deionized water, dried over anhydrous sodium sulfate, and filtered, and the solvent was then evaporated under reduced pressure to yield compounds **10a-t**. The compound **10u** was obtained by a simple reaction of the compound **10s** with methyl iodide in anhydrous DMF, and the compound **10v** was obtained by an acetylation reaction of compound **10s** with acetic anhydride.

N-(3,4,5-trimethoxyphenyl)-4-(4-methylphenyl)-1,3-thiazol-2-amine (**10a**). Yellow solid; yield: 81%; M.p.: 179–181 °C; ¹H-NMR (600 MHz, CDCl₃): δ 7.75 (d, *J* = 7.9 Hz, 2H), 7.19 (d, *J* = 7.9 Hz, 2H), 6.76 (s, 1H), 6.59 (s, 2H), 3.80 (s, 3H), 3.71 (s, 6H), 2.36 (s, 3H); ¹³C-NMR (150 MHz, CDCl₃): δ 165.6, 153.6 (2C), 151.0, 137.8, 136.7, 133.6, 131.7, 129.3 (2C), 126.0 (2C), 100.5 (2C), 96.2, 60.9, 55.8 (2C), 21.1; ESI-MS: *m/z* = 357.2 [M+H]⁺, 379.1 [M+Na]⁺.

N-(3,4,5-trimethoxyphenyl)-4-(4-methoxyphenyl)-1,3-thiazol-2-amine (**10b**). Brown solid; yield: 79%; M.p.: 65–67 °C; ¹H-NMR (600 MHz, CDCl₃): δ 7.77 (d, *J* = 8.7 Hz, 2H), 6.90 (d, *J* = 8.7 Hz, 2H), 6.66 (s, 1H), 6.62 (s, 2H), 3.82 (s, 3H), 3.81 (s, 3H), 3.77 (s, 6H); ¹³C-NMR (150 MHz, CDCl₃): δ 165.4, 159.4, 153.6 (2C), 150.6, 136.6, 133.7, 127.3 (2C), 127.2, 114.0 (2C), 99.5, 96.3 (2C), 60.9, 55.9 (2C), 55.2; ESI-MS: *m/z* = 373.2 [M+H]⁺, 395.1 [M+Na]⁺.

N-(3,4,5-trimethoxyphenyl)-4-(4-fluorophenyl)-1,3-thiazol-2-amine (**10c**). Pale brown solid; yield: 70%; M.p.: 134–136 °C; ¹H-NMR (600 MHz, CDCl₃): δ 7.80 (m, 2H), 7.06 (m, 2H), 6.73 (s, 1H), 6.64 (s, 2H), 3.82 (s, 3H), 3.81 (s, 6H); ¹³C-NMR (150 MHz, CDCl₃): δ 165.5, 162.5 (d, *J* = 248.0 Hz), 153.7 (2C), 150.0, 136.4, 133.9, 130.6 (d, *J* = 3.0 Hz), 127.7 (d, *J* = 8.0 Hz, 2C), 115.5 (d, *J* = 21.7 Hz, 2C), 101.0, 96.5 (2C), 61.0, 56.0 (2C); ESI-MS: *m/z* = 361.2 [M+H]⁺, 383.1 [M+Na]⁺, 399.1 [M+K]⁺.

N-(3,4,5-trimethoxyphenyl)-4-(4-chlorophenyl)-1,3-thiazol-2-amine (**10d**). Pale yellow solid; yield: 77%; M.p.: 149–151 °C; ¹H-NMR (600 MHz, CDCl₃): δ 7.77 (d, *J* = 8.5 Hz, 2H), 7.34 (d, *J* = 8.5 Hz, 2H), 6.79 (s, 1H), 6.61 (s, 2H), 3.82 (s, 3H), 3.77 (s, 6H); ¹³C-NMR (150 MHz, CDCl₃): δ 165.7, 153.7 (2C), 149.9, 136.4, 133.9, 133.6, 132.9, 128.8 (2C), 127.2 (2C), 101.8, 96.5 (2C), 61.0, 55.9 (2C); ESI-MS: *m/z* = 377.1 [M+H]⁺, 399.1 [M+Na]⁺.

N-(3,4,5-trimethoxyphenyl)-4-(4-bromophenyl)-1,3-thiazol-2-amine (**10e**). Yellow solid; yield: 82%; M.p.: 144–146 °C; ¹H-NMR (600 MHz, CDCl₃): δ 7.69 (d, *J* = 8.4 Hz, 2H), 7.51 (d, *J* = 8.4 Hz, 2H), 6.79 (s, 1H), 6.65 (s, 2H), 3.83 (s, 9H); ¹³C-NMR (150 MHz, CDCl₃): δ 165.6, 153.7 (2C), 149.9, 136.3, 134.0, 133.2, 131.7 (2C), 127.5 (2C), 121.8, 101.9, 96.6 (2C), 61.0, 56.0 (2C); ESI-MS: *m/z* = 421.0 [M+H]⁺.

N-(3,4,5-trimethoxyphenyl)-4-(4-nitrophenyl)-1,3-thiazol-2-amine (**10f**). Orange solid; yield: 73%; M.p.: 98–99 °C; ¹H-NMR (600 MHz, CDCl₃): δ 8.32 (d, *J* = 8.0 Hz, 2H), 7.57 (d, *J* = 8.0 Hz, 2H), 6.36 (s, 2H), 5.99 (s, 1H), 3.84 (s, 9H); ¹³C-NMR (150 MHz, CDCl₃): δ 160.1, 153.8 (2C), 147.9, 138.4, 137.5, 133.9, 129.1 (2C), 126.4, 124.1 (2C), 98.7, 98.3 (2C), 60.9, 55.9 (2C); ESI-MS: *m/z* = 388.2 [M+H]⁺, 410.2 [M+Na]⁺.

N-(3,4,5-trimethoxyphenyl)-4-(3,4-dimethoxyphenyl)-1,3-thiazol-2-amine (**10g**). Brown solid; yield: 75%; M.p.: 54–56 °C; ¹H-NMR (600 MHz, CDCl₃): δ 7.38 (m, 2H), 6.88 (d, *J* = 8.7 Hz, 1H), 6.67 (s, 1H), 6.66 (s, 2H), 3.92 (s, 3H), 3.90 (s, 3H), 3.82 (s, 9H); ¹³C-NMR (150 MHz, CDCl₃): δ 165.4, 153.7 (2C), 150.1, 149.1, 148.9, 136.2, 134.0, 127.0, 118.5, 111.2, 109.3, 99.7, 96.5 (2C), 60.9, 56.0 (2C), 55.9, 55.8; ESI-MS: *m/z* = 403.2 [M+H]⁺, 425.1 [M+Na]⁺.

N-(3,4,5-trimethoxyphenyl)-4-(3-fluoro-4-methoxyphenyl)-1,3-thiazol-2-amine (**10h**). Brown red solid; yield: 76%; M.p.: 148–150 °C; ¹H-NMR (600 MHz, CDCl₃): δ 7.56 (s, 1H), 7.54 (s, 1H), 6.93–6.96 (m, 1H), 6.67 (s, 1H), 6.65 (s, 2H), 3.90 (s, 3H), 3.82 (s, 3H), 3.80 (s, 6H); ¹³C-NMR (150 MHz, CDCl₃): δ 165.5, 153.6 (2C), 152.3 (d, *J* = 245.0 Hz), 149.6, 147.4 (d, *J* = 10.8 Hz),

136.4, 133.8, 127.9 (d, $J = 6.9$ Hz), 121.8 (d, $J = 2.2$ Hz), 113.8 (d, $J = 19.7$ Hz), 113.3, 100.6, 96.5 (2C), 60.9, 56.2, 55.9 (2C); ESI-MS: $m/z = 391.2$ [M+H]⁺, 413.2 [M+Na]⁺, 429.1 [M+K]⁺.

N-(3,4,5-trimethoxyphenyl)-4-(3-nitro-4-methoxyphenyl)-1,3-thiazol-2-amine (**10i**). Yellow solid; yield: 84%; M.p.: 173–174 °C; ¹H-NMR (600 MHz, CDCl₃): δ 8.35 (d, $J = 1.5$ Hz, 1H), 7.94 (dd, $J = 8.7$ Hz, $J = 1.5$ Hz, 2H), 7.08 (d, $J = 8.7$ Hz, 1H), 6.76 (s, 1H), 6.75 (s, 2H), 3.97 (s, 3H), 3.86 (s, 6H), 3.83 (s, 3H); ¹³C-NMR (150 MHz, CDCl₃): δ 165.2, 153.7 (2C), 152.4, 148.5, 139.4, 136.3, 133.9, 131.2, 127.4, 123.4, 113.6, 101.6, 96.3 (2C), 61.0, 56.6, 56.0 (2C); ESI-MS: $m/z = 418.2$ [M+H]⁺.

N-(3,4,5-trimethoxyphenyl)-4-(3-amino-4-methoxyphenyl)-1,3-thiazol-2-amine (**10j**). Yellow solid; yield: 65%; M.p.: 166–167 °C; ¹H-NMR (600 MHz, CDCl₃): δ 7.20 (m, 2H), 6.79 (d, $J = 8.1$ Hz, 1H), 6.62 (s, 2H), 6.61 (s, 1H), 3.87 (s, 3H), 3.81 (s, 3H), 3.79 (s, 6H); ¹³C-NMR (150 MHz, CDCl₃): δ 165.4, 153.6 (2C), 151.0, 147.3, 136.6, 136.1, 133.7, 127.5, 116.5, 112.7, 110.3, 99.5, 96.4 (2C), 60.9, 55.9 (2C), 55.5; ESI-MS: $m/z = 388.2$ [M+H]⁺, 410.2 [M+Na]⁺.

N-(3,4,5-trimethoxyphenyl)-4-(3-benzyloxy-4-methoxyphenyl)-1,3-thiazol-2-amine (**10k**). Red solid; yield: 74%; M.p.: 77–78 °C; ¹H-NMR (600 MHz, DMSO-*d*₆): δ 10.20 (s, 1H), 7.61 (d, $J = 2.0$ Hz, 1H), 7.51 (dd, $J = 8.3$ Hz, $J = 2.0$ Hz, 1H), 7.49 (d, $J = 7.3$ Hz, 2H), 7.41 (m, 2H), 7.35 (d, $J = 7.3$ Hz, 1H), 7.19 (s, 1H), 7.16 (s, 2H), 7.03 (d, $J = 8.3$ Hz, 1H), 5.12 (s, 2H), 3.82 (s, 6H), 3.80 (s, 3H), 3.63 (s, 3H); ¹³C-NMR (150 MHz, DMSO-*d*₆): δ 163.3, 153.4 (2C), 150.3, 149.3, 148.2, 137.9, 137.4, 132.2, 128.8 (2C), 128.3 (2C), 128.0, 119.0, 112.6, 111.6, 111.6, 101.3, 95.0 (2C), 70.4, 60.5, 56.0, 56.0 (2C); ESI-MS: $m/z = 479.2$ [M+H]⁺, 501.1 [M+Na]⁺, 517.1 [M+K]⁺.

N-(3,4,5-trimethoxyphenyl)-4-(3-hydroxy-4-methoxyphenyl)-1,3-thiazol-2-amine (**10l**). Red solid; yield: 73%; M.p.: 98–100 °C; ¹H-NMR (600 MHz, CDCl₃): δ 7.37 (d, $J = 1.9$ Hz, 1H), 7.36 (dd, $J = 8.3$ Hz, $J = 1.9$ Hz, 2H), 6.85 (d, $J = 8.3$ Hz, 1H), 6.65 (s, 2H), 6.64 (s, 1H), 3.90 (s, 3H), 3.82 (s, 6H), 3.82 (s, 3H); ¹³C-NMR (150 MHz, CDCl₃): δ 165.3, 153.6 (2C), 150.5, 146.6, 145.6, 136.6, 133.7, 128.0, 118.1, 112.3, 110.7, 100.0, 96.4 (2C), 60.9, 56.0 (2C), 55.9; ESI-MS: $m/z = 389.1$ [M+H]⁺, 777.3 [2M+H]⁺, 799.3 [2M+Na]⁺.

N-(3,4,5-trimethoxyphenyl)-4-(3,4-difluorophenyl)-1,3-thiazol-2-amine (**10m**). Yellow solid; yield: 64%; M.p.: 153–155 °C; ¹H-NMR (600 MHz, CDCl₃): δ 7.70–7.71 (m, 1H), 7.62–7.65 (m, 1H), 7.14–7.18 (m, 1H), 6.74 (s, 1H), 6.70 (s, 2H), 3.86 (s, 6H), 3.83 (s, 3H); ¹³C-NMR (150 MHz, CDCl₃): δ 165.3, 153.7 (2C), 149.0, 136.3, 134.0, 132.2, 130.9, 128.8, 121.8, 117.4 (d, $J = 16.8$ Hz), 115.0 (d, $J = 18.9$ Hz), 102.0, 96.5 (2C), 61.0, 56.0 (2C); ESI-MS: $m/z = 379.1$ [M+H]⁺.

N-(3,5-dimethoxyphenyl)-4-(4-methoxyphenyl)-1,3-thiazol-2-amine (**10n**). Pale yellow solid; yield: 63%; M.p.: 150–151 °C; ¹H-NMR (600 MHz, CDCl₃): δ 7.79 (d, $J = 8.7$ Hz, 2H), 6.91 (d, $J = 8.7$ Hz, 2H), 6.71 (s, 1H), 6.51 (d, $J = 2.1$ Hz, 1H), 6.15 (m, 1H), 3.82 (s, 3H), 3.70 (s, 6H); ¹³C-NMR (150 MHz, CDCl₃): δ 164.5, 161.4 (2C), 159.4, 150.6, 142.1, 130.2, 127.3 (2C), 114.0 (2C), 100.1, 96.2 (2C), 95.1, 55.2, 55.2 (2C); ESI-MS: $m/z = 343.2$ [M+H]⁺, 365.2 [M+Na]⁺.

N-(4-methoxyphenyl)-4-(3,4,5-trimethoxyphenyl)-1,3-thiazol-2-amine (**10o**). Khaki solid; yield: 66%; M.p.: 66–68 °C; ¹H-NMR (600 MHz, CDCl₃): δ 7.20 (d, $J = 8.8$ Hz, 2H), 7.02 (s, 2H), 6.82 (d, $J = 8.8$ Hz, 2H), 6.63 (s, 1H), 3.84 (s, 6H), 3.83 (s, 3H), 3.77 (s, 3H); ¹³C-NMR (150 MHz, CDCl₃): δ 167.4, 156.3, 153.2 (2C), 137.9, 133.6, 130.3, 121.9 (2C), 114.7, 114.5 (2C), 103.4 (2C), 100.5, 60.8, 56.0 (2C), 55.4; ESI-MS: $m/z = 373.2$ [M+H]⁺, 395.1 [M+Na]⁺.

N-(3,4-dimethoxyphenyl)-4-(3-nitro-4-methoxyphenyl)-1,3-thiazol-2-amine (**10p**). Red solid; yield: 63%; M.p.: 166–167 °C; ¹H-NMR (600 MHz, CDCl₃): δ 8.27 (s, 1H), 7.94 (d, $J = 8.7$ Hz, 1H), 7.08 (s, 2H), 7.01 (m, 2H), 6.70 (s, 1H), 3.93 (s, 3H), 2.22 (s, 3H), 2.20 (s, 3H); ¹³C-NMR (150 MHz, CDCl₃): δ 166.3, 152.2, 148.4, 139.4, 137.8, 137.8, 132.1, 131.6, 130.4, 127.5, 123.2, 120.7, 116.5, 113.5, 101.4, 56.5, 19.9, 19.0; ESI-MS: $m/z = 356.1$ [M+H]⁺, 378.1 [M+Na]⁺.

N-(3,4-dimethoxyphenyl)-4-(3-amino-4-methoxyphenyl)-1,3-thiazol-2-amine (**10q**). Brown solid; yield: 68%; M.p.: 146–148 °C; ¹H-NMR (600 MHz, CDCl₃): δ 7.18 (s, 1H), 7.16 (m, 1H), 7.09 (m, 2H), 7.06 (s, 1H), 6.76 (d, $J = 8.8$ Hz, 1H), 6.55 (s, 1H), 3.85 (s, 3H), 2.23 (s, 3H), 2.22

(s, 3H); ^{13}C -NMR (150 MHz, CDCl_3): δ 165.8, 150.4, 147.3, 138.0, 137.7, 136.1, 131.7, 130.3, 127.3, 120.5, 116.5, 116.3, 112.9, 110.3, 99.2, 55.5, 19.9, 19.0; ESI-MS: m/z = 326.1 $[\text{M}+\text{H}]^+$, 348.1 $[\text{M}+\text{Na}]^+$, 364.0 $[\text{M}+\text{K}]^+$.

N-(2,4-dimethoxyphenyl)-4-(4-methoxyphenyl)-1,3-thiazol-2-amine (**10r**). Brown solid; yield: 75%; M.p.: 65–66°C; ^1H -NMR (600 MHz, CDCl_3): δ 7.91 (d, J = 8.4 Hz, 1H), 7.75 (d, J = 8.0 Hz, 2H), 7.21 (d, J = 8.0 Hz, 2H), 6.71 (s, 1H), 6.54 (m, 2H), 3.87 (s, 3H), 3.82 (s, 3H), 2.38 (s, 3H); ^{13}C -NMR (150 MHz, CDCl_3): δ 165.1, 155.8, 151.1, 149.6, 137.5, 131.8, 129.2 (2C), 125.9 (2C), 123.7, 118.6, 103.7, 100.4, 99.1, 55.7, 55.5, 21.2; ESI-MS: m/z = 327.2 $[\text{M}+\text{H}]^+$, 349.1 $[\text{M}+\text{Na}]^+$.

N-(2,4-dimethoxyphenyl)-4-(4-methoxyphenyl)-1,3-thiazol-2-amine (**10s**). Brown red solid; yield: 80%; M.p.: 98–99°C; ^1H -NMR (600 MHz, CDCl_3): δ 7.92 (d, J = 8.4 Hz, 1H), 7.79 (d, J = 8.7 Hz, 2H), 6.93 (d, J = 8.7 Hz, 2H), 6.62 (s, 1H), 6.53 (m, 2H), 3.85 (s, 3H), 3.83 (s, 3H), 3.81 (s, 3H); ^{13}C -NMR (150 MHz, CDCl_3): δ 165.0, 159.2, 155.7, 151.0, 149.5, 127.7, 127.3 (2C), 123.8, 118.5, 113.8 (2C), 103.7, 99.4, 99.1, 55.6, 55.5, 55.2; ESI-MS: m/z = 343.2 $[\text{M}+\text{H}]^+$, 365.1 $[\text{M}+\text{Na}]^+$, 381.1 $[\text{M}+\text{K}]^+$.

N-(2,4-dimethoxyphenyl)-4-(2,4-dimethoxyphenyl)-1,3-thiazol-2-amine (**10t**). Brown solid; yield: 65%; M.p.: 151–153°C; ^1H -NMR (600 MHz, CDCl_3): δ 8.13 (d, J = 8.4 Hz, 1H), 7.95 (d, J = 8.5 Hz, 1H), 7.13 (s, 1H), 6.59 (dd, J = 8.5 Hz, J = 1.9 Hz, 1H), 6.53 (m, 3H), 3.91 (s, 3H), 3.86 (s, 3H), 3.84 (s, 3H), 3.81 (s, 3H); ^{13}C -NMR (150 MHz, CDCl_3): δ 163.1, 160.0, 157.9, 155.5, 149.3, 146.8, 130.7, 124.0, 118.2, 116.8, 104.5, 104.0, 103.7, 99.0, 98.6, 55.6, 55.5, 55.3, 55.3; ESI-MS: m/z = 373.2 $[\text{M}+\text{H}]^+$, 395.1 $[\text{M}+\text{Na}]^+$.

N-(2,4-dimethoxyphenyl)-4-(4-methoxyphenyl)-*N*-methyl-1,3-thiazol-2-amine (**10u**). NaH (5.4 mmol) was added to a stirred solution of **10s** (2.8 mmol) in DMF (5 mL), and the mixture was stirred at 25°C for 2 min. MeI (2.8 mmol) was added dropwise, and the mixture was stirred at 25°C for 1 h. The reaction was quenched with saturated aqueous NH_4Cl solution (15 mL), and the mixture was extracted with EtOAc (3×15 mL). The combined organic fraction was dried and the solvent was evaporated. The crude solid was purified by column chromatography to yield **10u**. White solid; yield: 53%; M.p.: 126–128°C; ^1H -NMR (600 MHz, CDCl_3): δ 7.81 (d, J = 8.8 Hz, 2H), 7.27 (s, 1H), 6.92 (d, J = 8.8 Hz, 2H), 6.58 (d, J = 2.6 Hz, 1H), 6.52 (dd, J = 8.6 Hz, J = 2.6 Hz, 1H), 6.48 (s, 1H), 3.85 (s, 3H), 3.84 (s, 3H), 3.80 (s, 3H), 1.27 (s, 3H); ^{13}C -NMR (150 MHz, CDCl_3): δ 171.6, 160.4, 158.9, 156.9, 151.2, 130.1, 128.4, 127.7, 127.2 (2C), 113.7 (2C), 104.7, 100.2, 99.7, 55.6, 55.5, 55.2, 39.3; ESI-MS: m/z = 357.2 $[\text{M}+\text{H}]^+$, 379.1 $[\text{M}+\text{Na}]^+$, 395.1 $[\text{M}+\text{K}]^+$.

N-(2,4-dimethoxyphenyl)-4-(4-methoxyphenyl)-*N*-acetyl-1,3-thiazol-2-amine (**10v**). A flask immersed in a room temperature oil bath was charged with **10s** (2 mmol) and Ac_2O (10 mL) and heated to 50°C. After completion of the reaction, the reaction was quenched upon addition of 50 g of ice. A yellow precipitate formed, which was filtered and washed with H_2O . The crude solid was purified by column chromatography to give pure **10v**. Yellow solid; yield: 54%; M.p.: 146–148°C; ^1H -NMR (600 MHz, CDCl_3): δ 7.58 (d, J = 8.8 Hz, 2H), 7.22 (d, J = 9.2 Hz, 1H), 7.03 (s, 1H), 6.82 (d, J = 8.8 Hz, 2H), 6.60 (m, 2H), 3.89 (s, 3H), 3.77 (s, 3H), 3.74 (s, 3H), 2.06 (s, 3H); ^{13}C -NMR (150 MHz, CDCl_3): δ 171.0, 161.2, 159.1, 155.9, 148.8, 130.7, 127.8, 127.1 (2C), 122.2, 113.7 (2C), 106.5, 104.8, 99.6, 55.7, 55.5, 55.2, 22.9; ESI-MS: m/z = 385.2 $[\text{M}+\text{H}]^+$, 407.1 $[\text{M}+\text{Na}]^+$.

Biology

MTT assay: The SGC-7901, A549 and HT-1080 cell lines were purchased from the American Type Culture Collection (ATCC, Manassas, VA, USA). The in vitro antiproliferative activities of CA-4 (**2**), Nocodazole (**3**) and all of the target compounds were determined with an MTT assay following a previously reported method [21,22].

Tubulin assembly assay: The effect of **10s** on the polymerization of purified brain tubulin was determined using a fluorescence-based tubulin polymerization assay kit (Cat. #BK011P, Cytoskeleton, Inc., USA) following a previously reported method [22].

Immunofluorescence assay: Immunostaining was performed to detect the microtubule-associated tubulin protein after exposure to CA-4 (**2**) or the investigated compound **10s** following a previously reported method [21,22].

Cell cycle analysis: SGC-7901 cells (8×10^4 cells) were incubated with various concentrations of CA-4 (**2**), **10s** or 0.05% DMSO for the indicated times. The cells were collected by centrifugation, washed with PBS and fixed in ice-cold 70% ethanol. The fixed cells were harvested by centrifugation and resuspended in 500 μ l of PBS containing 1 mg/mL RNase. After 30 min of incubation at 37°C, the cells were stained with 50 mg/mL propidium iodide (PI) at 4°C in the dark for 30 min. The samples were then analyzed by FACScan flow cytometry (Becton-Dickinson, Franklin Lakes, NJ, USA). The experiments were repeated at least three times.

Molecular modeling: The molecular modeling studies were performed using Accelrys Discovery Studio 3.0. The crystal structure of tubulin complexed with DAMA-colchicine (PDB: 3HKD) was retrieved from the RCSB Protein Data Bank (<http://www.rcsb.org/pdb>). In the docking process, the protein protocol was prepared via several operations, including the standardization of atom names, insertion of missing atoms in residues and removal of alternate conformations, insertion of missing loop regions based on SEQRES data, optimization of short and medium sized loop regions with the Looper Algorithm, minimization of remaining loop regions, calculation of pK, and protonation of the structure. The receptor model was then typed with the CHARMM force field, and a binding sphere with a radius of 9.0 Å was defined with the original ligand (DAMA-colchicine) as the binding site. The **10s** was drawn with Chemdraw and fully minimized using the CHARMM force field. Finally, **10s** was docked into the binding site using the CDocker protocol with the default settings.

QSAR Model: In the model, 80% of the target compounds were utilized as a training set for QSAR modeling. The remaining 20% were chosen as a test subset using the same protocol. The literature-based inhibitory activity values of the known compounds [IC_{50} of SGC-7901 cells] were initially converted into the minus logarithmic scale [pIC_{50}] and then used for subsequent QSAR analysis as the response variable. In Discovery Studio, the CHARMM force field was applied and the electrostatic potential together with the Van der Waals potential were treated as separate terms. As the electrostatic potential probe, A+ le point change was used while distance-dependent dielectric constant was used to mimic the solvent effect. A carbon atom with a radius of 1.73 Å was used as a probe for the Van der Waals potential. A Partial Least-Squares (PLS) model was built using energy grids as descriptors. QSAR models were built by using the Create 3D QSAR Model protocol in Discovery Studio 3.0.

Supporting information

S1 File. (1). Synthesis. 1. General synthetic procedures for aryl thioamides 14. 2. General synthetic procedures for α -bromoacetophenones 16. **(2). Contents:** 1H-NMR and 13C-NMR spectra of all target compounds. (PDF)

Acknowledgments

This work was supported by the Programme for Innovative Research Team of the Ministry of Education and the Programme for Liaoning Innovative Research Team in University.

Author Contributions

Conceptualization: MS QX WZ.

Data curation: MS QX JX.

Formal analysis: MS QX WZ.

Funding acquisition: WZ.

Investigation: MS QX WZ.

Methodology: MS QX JX Yue Wu Y. Wang.

Project administration: WZ.

Resources: MS QX WZ.

Software: QX Yue Wu JW.

Supervision: KB WZ.

Validation: DZ QG KB JW Yingliang Wu.

Visualization: MS QX KB WZ.

Writing – original draft: QX.

Writing – review & editing: MS QX KB WZ.

References

1. Stephens RE, Edds KT. Microtubules: structure, chemistry, and function. *Physiol Rev.* 1976; 56(4): 709–777. PMID: [790425](#)
2. Etienne-Manneville S. From signaling pathways to microtubule dynamics: the key players. *Curr Opin Cell Biol.* 2010; 22(1): 104–111. <https://doi.org/10.1016/j.ceb.2009.11.008> PMID: [20031384](#)
3. Kavallaris M. Microtubules and resistance to tubulin-binding agents. *Nat Rev Cancer.* 2010; 10(3): 194–204. <https://doi.org/10.1038/nrc2803> PMID: [20147901](#)
4. Dumontet C, Jordan MA. Microtubule-binding agents: a dynamic field of cancer therapeutics. *Nat Rev Drug Discov.* 2010; 9(10): 790–803. <https://doi.org/10.1038/nrd3253> PMID: [20885410](#)
5. Jordan MA, Wilson L. Microtubules as a target for anticancer drugs. *Nat Rev Cancer.* 2004; 4(4): 253–265. <https://doi.org/10.1038/nrc1317> PMID: [15057285](#)
6. Dong M, Liu F, Zhou H, Zhai S, Yan B. Novel Natural Product- and Privileged Scaffold-Based Tubulin Inhibitors Targeting the Colchicine Binding Site. *Molecules.* 2016; 21(10): 1375–1401.
7. Carlson RO. New tubulin targeting agents currently in clinical development. *Expert Opin Investig Drugs.* 2008; 17(5): 707–722. <https://doi.org/10.1517/13543784.17.5.707> PMID: [18447597](#)
8. Graening T, Schmalz HG. Total syntheses of colchicine in comparison: a journey through 50 years of synthetic organic chemistry. *Angew Chem Int Ed Engl.* 2004; 43(25): 3230–3256. <https://doi.org/10.1002/anie.200300615> PMID: [15213947](#)
9. Pettit GR, Singh SB, Niven ML, Hamel E, Schmidt JM. Isolation, structure, and synthesis of combretastatins A-1 and B-1, potent new inhibitors of microtubule assembly, derived from *Combretum caffrum*. *J Nat Prod.* 1987; 50(1): 119–131. PMID: [3598594](#)
10. Pettit GR, Singh SB, Hamel E, Lin CM, Alberts DS, Garcia-Kendall D. Isolation and structure of the strong cell growth and tubulin inhibitor combretastatin A-4. *Experientia.* 1989; 45(2): 209–211. PMID: [2920809](#)
11. Chaudhary A, Pandeya SN, Kumar P, Sharma PP, Gupta S, Soni N, et al. Combretastatin a-4 analogs as anticancer agents. *Mini Rev Med Chem.* 2007; 7(12): 1186–1205. PMID: [18220974](#)
12. Attia SM. Molecular cytogenetic evaluation of the mechanism of genotoxic potential of amsacrine and nocodazole in mouse bone marrow cells. *J Appl Toxicol.* 2013; 33(6): 426–433. <https://doi.org/10.1002/jat.1753> PMID: [22081495](#)

13. Pettit GR, Toki B, Herald DL, Verdier-Pinard P, Boyd MR, Hamel E, et al. Antineoplastic agents. 379. Synthesis of phenstatin phosphate. *J Med Chem.* 1998; 41(10): 1688–1695. <https://doi.org/10.1021/jm970644q> PMID: 9572894
14. Lu Y, Li CM, Wang Z, Ross CR, Chen J, Dalton JT, et al. Discovery of 4-substituted methoxybenzoyl-aryl-thiazole as novel anticancer agents: synthesis, biological evaluation, and structure-activity relationships. *J Med Chem.* 2009; 52(6): 1701–1711. <https://doi.org/10.1021/jm801449a> PMID: 19243174
15. Chen J, Wang Z, Li CM, Lu Y, Vaddady PK, Meibohm B, et al. Discovery of novel 2-aryl-4-benzoyl-imidazoles targeting the colchicines binding site in tubulin as potential anticancer agents. *J Med Chem.* 2010; 53(20): 7414–7427. <https://doi.org/10.1021/jm100884b> PMID: 20919720
16. Xiao M, Ahn S, Wang J, Chen J, Miller DD, Dalton JT, et al. Discovery of 4-Aryl-2-benzoyl-imidazoles as tubulin polymerization inhibitor with potent antiproliferative properties. *J Med Chem.* 2013; 56(8): 3318–3329. <https://doi.org/10.1021/jm4001117> PMID: 23547728
17. La Regina G, Bai R, Coluccia A, Famigliani V, Pelliccia S, Passacantilli S, Mazzoccoli C, et al. New Pyrrole Derivatives with Potent Tubulin Polymerization Inhibiting Activity As Anticancer Agents Including Hedgehog-Dependent Cancer. *J Med Chem.* 2014; 57(15): 6531–6552. <https://doi.org/10.1021/jm500561a> PMID: 25025991
18. Guan Q, Feng D, Bai Z, Cui Y, Zuo D, Zhai M, et al. Microwave-assisted synthesis, molecular docking and antiproliferative activity of (3/5-aryl-1,2,4-oxadiazole-5/3-yl)(3,4,5-trimethoxyphenyl)methanone oxime derivatives. *Med Chem Comm.* 2015; 6(8): 1484–1493.
19. Kim KS, Kimball SD, Misra RN, Rawlins DB, Hunt JT, Xiao HY, et al. Discovery of Aminothiazole Inhibitors of Cyclin-Dependent Kinase 2: Synthesis, X-ray Crystallographic Analysis, and Biological Activities. *J. Med. Chem.* 2002; 45(18): 3905–3927. PMID: 12190313
20. Wang XF, Ohkoshi E, Wang SB, Hamel E, Bastow KF, Morris-Natschke SL, et al. Synthesis and biological evaluation of *N*-alkyl-*N*-(4-methoxyphenyl)pyridin-2-amines as a new class of tubulin polymerization inhibitors. *Bioorg. Med. Chem.* 2013; 21(3): 632–642. <https://doi.org/10.1016/j.bmc.2012.11.047> PMID: 23274123
21. Guan Q, Yang F, Guo D, Xu J, Jiang M, Liu C, et al. Synthesis and biological evaluation of novel 3,4-diaryl-1,2,5-selenadiazol analogues of combretastatin A-4. *Eur J Med Chem.* 2014; 87: 1–9. <https://doi.org/10.1016/j.ejmech.2014.09.046> PMID: 25233100
22. Xu Q, Qi H, Sun M, Zuo D, Jiang X, Wen Z; et al. Synthesis and Biological Evaluation of 3-Alkyl-1,5-Diaryl-1H-Pyrazoles as Rigid Analogues of Combretastatin A-4 with Potent Antiproliferative Activity. *PLoS One.* 2015; 10(6): e0128710. <https://doi.org/10.1371/journal.pone.0128710> PMID: 26061410
23. Das D, Sikdar P, Bairagi M. Recent developments of 2-aminothiazoles in medicinal chemistry. *Eur J Med Chem.* 2016; 109: 89–98. <https://doi.org/10.1016/j.ejmech.2015.12.022> PMID: 26771245
24. Taguchi M, Kondo H, Inoue Y, Kawahata Y, Jinbo Y, Sakamoto F, et al. Synthesis and antibacterial activity of new tetracyclic quinolone antibacterials. *J Med Chem.* 1992; 35(1): 94–99. PMID: 1310116
25. Jiang Z, Chen Y, Yang C, Cao Y, Tao Y, Qin J, et al. A fully diarylmethylene-bridged triphenylamine derivative as novel host for highly efficient green phosphorescent OLEDs. *Org Lett.* 2009; 11(7): 1503–1506. <https://doi.org/10.1021/ol9001152> PMID: 19256517
26. Kabalka GW, Mereddy AR. Microwave promoted synthesis of functionalized 2-aminothiazoles. *Tetrahedron Letters.* 2006; 47: 5171–5172.
27. Sato T, Tomaru K, Koide T, Masuda M, Yamamoto M, Miyazawa N; et al. Synchronous lung and gastric cancers successfully treated with carboplatin and pemetrexed: a case report. *J Med Case Rep.* 2012; 6: 266. <https://doi.org/10.1186/1752-1947-6-266> PMID: 22938085
28. Rasheed S, Nelson-Rees WA, Toth EM, Arnstein P, Gardner MB. Characterization of a newly derived human sarcoma cell line (HT-1080). *Cancer.* 1974; 33(4): 1027–1033. PMID: 4132053